

## Selective Synthesis of (9,8) Single Walled Carbon Nanotubes on Cobalt Incorporated TUD-1 Catalysts

Hong Wang,<sup>†</sup> Bo Wang,<sup>†,‡</sup> Xian-Yang Quek,<sup>†</sup> Li Wei,<sup>†</sup> Jianwen Zhao,<sup>§</sup> Lain-Jong Li,<sup>||</sup>  
Mary B. Chan-Park,<sup>†</sup> Yanhui Yang,<sup>\*,†</sup> and Yuan Chen<sup>\*,†</sup>

School of Chemical and Biomedical Engineering, Nanyang Technological University, Singapore 637459, Institute of Chemical and Engineering Sciences, Singapore 627833, School of Materials Science and Engineering, Nanyang Technological University, Singapore 639798, and Research Center for Applied Science, Academia Sinica, Taiwan

Received August 3, 2010; E-mail: chenyan@ntu.edu.sg; yhyang@ntu.edu.sg

**Abstract:** Selective synthesis of single walled carbon nanotubes (SWCNTs) with specific  $(n,m)$  structures is desired for many potential applications. Current chirality control growth has only achieved at small diameter (6,5) and (7,5) nanotubes. Each  $(n,m)$  species is a distinct molecule with structure-dependent properties; therefore it is essential to extend chirality control to various  $(n,m)$  species. In this communication, we demonstrate the highly selective synthesis of (9,8) nanotubes on a cobalt incorporated TUD-1 catalyst are (Co-TUD-1). When catalysts were pre-reduced in H<sub>2</sub> at the optimized temperature of 500 °C, 59.1% of semi-conducting nanotubes have the (9,8) structure. The uniqueness of Co-TUD-1 relies on its low reduction temperature (483 °C), large surface area, and strong metal–support interaction, which stabilizes Co clusters responsible for the growth of (9,8) nanotubes. SWCNT thin film field effect transistors fabricated using (9,8) nanotubes from our synthesis process have higher average device mobility and a higher fraction of semiconducting devices than those using (6,5) nanotubes. Combining with further postsynthetic sorting techniques, our selective synthesis method brings us closer to the ultimate goal of producing  $(n,m)$  specific nanotube materials.

Selective synthesis of single walled carbon nanotubes (SWCNTs) with specific  $(n,m)$  structures is desired for many potential applications.<sup>1</sup> Current synthesis methods generally produce SWCNTs with random  $(n,m)$  distributions. In a few cases, Co–Mo, Fe/Co-zeolite, Co-MCM-41, Fe–Ru, Fe–Ni, and Au catalysts have synthesized SWCNTs with a narrow  $(n,m)$  distribution.<sup>2</sup> Notably, chirality control has only achieved at small diameter (6,5) and (7,5) nanotubes. These catalysts lose their  $(n,m)$  selectivity when the SWCNT diameter increases. Each  $(n,m)$  species is a distinct molecule with structure-dependent properties; therefore, it is essential to extend chirality control to various  $(n,m)$  species.<sup>3</sup>

In this communication, we demonstrate the selective synthesis of (9,8) nanotubes on a cobalt incorporated TUD-1 catalyst (Co-TUD-1). The chirality distribution was analyzed by photoluminescence excitation/emission (PLE) spectroscopy, UV–vis–NIR absorption spectroscopy, and Raman scattering spectroscopy with multilaser excitation. The catalyst pre-reduction temperature under H<sub>2</sub> was found to be a critical parameter in chirality control. Moreover, the electronic characteristics of (9,8) nanotubes were

compared with those of (6,5) nanotubes from a Co–Mo catalyst using SWCNT thin film field effect transistors (FETs).

TUD-1 is a mesoporous silica matrix with a large surface area and high thermal stability. Metal ions can be incorporated into the silica matrix, which makes TUD-1 a good catalyst candidate.<sup>4</sup> Co-TUD-1 with 1 wt % Co was synthesized (see Supporting Information (SI) for details). Physicochemical properties of Co-TUD-1 were characterized by X-ray diffraction, nitrogen physisorption, UV–vis spectroscopy, and H<sub>2</sub> temperature programmed reduction (TPR) and was presented in the SI. Co-TUD-1 possesses a well-defined mesoporous structure, large surface area (740 m<sup>2</sup>/g), pore volume (1.42 mL/g), and narrow pore size distribution centered at 7.4 nm (see Figure S1, SI). Co<sup>2+</sup> ions are incorporated at tetrahedral sites in the TUD-1 matrix or on its surface with a distinct and narrow reduction peak at 483 °C (see Figure S2, SI). SWCNTs were synthesized in a pressured CO chemical vapor deposition reactor. Co-TUD-1 catalysts were initially pre-reduced at a certain temperature under H<sub>2</sub> (1 bar, 50 sccm) for 0.5 h. Subsequently, the reactor temperature was increased to 800 °C under Ar flow, and eventually CO (6 bar, 100 sccm) was introduced at 800 °C for 1 h. As-synthesized SWCNTs were refluxed in 1.5 mol/L NaOH solvent to dissolve the TUD-1 matrix. The remaining carbon deposits were dispersed in 2 wt % sodium dodecyl benzene sulfonate (SDBS) D<sub>2</sub>O (Aldrich) solution by sonication in an ultrasonicator (Sonics, VCX-130) at 20 W for 0.5 h. After sonication, the suspension was

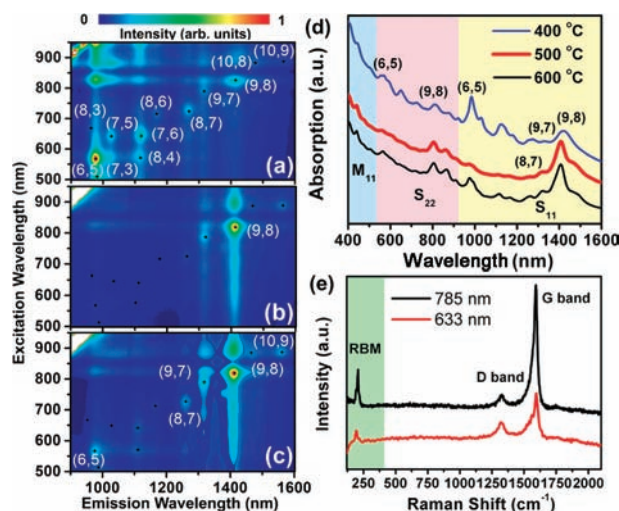


**Figure 1.** PLE maps of SDBS-dispersed SWCNTs produced from Co-TUD-1 after pre-reduction under H<sub>2</sub> at different temperatures: (a) 400, (b) 500, and (c) 600 °C. (d) UV–vis–NIR spectra of SWCNTs. (e) Raman spectra of as-synthesized SWCNTs grown after 500 °C pre-reduction using the excitation laser wavelengths of 633 and 785 nm.

<sup>†</sup> School of Chemical and Biomedical Engineering, Nanyang Technological University.

<sup>‡</sup> Institute of Chemical and Engineering Sciences.

<sup>§</sup> School of Materials Science and Engineering, Nanyang Technological University.

<sup>||</sup> Academia Sinica.

centrifuged at 50 000 *g* for 1 h to remove metal particles, undispersed nanotube bundles, and other carbon impurities. Clear and stable SWCNT suspensions obtained after centrifugation were characterized by PLE and UV–vis–NIR spectroscopy.

Figure 1a to 1c show PLE maps of SWCNTs produced from Co-TUD-1. The resonance behavior of excitation and emission events yield peaks corresponding to transition pairs from individual semiconducting (*n,m*) species.<sup>5</sup> The relative abundance of every species was calculated based on their PLE peak intensities, and the findings are listed in Tables S1 to S3, SI. Figure 1b shows a high selectivity toward (9,8) nanotubes after prereluction at 500 °C, in which 59.1% of semiconducting nanotubes are (9,8) (Table S2, SI). At a prereluction temperature of 400 °C, (6,5) have the highest PLE intensity with 32.6% abundance (Figure 1a and Table S1, SI). In contrast, (10,9), (9,8), (9,7), and (6,5) were produced after prereluction at 600 °C with abundances of 7.4%, 43.5%, 12.3%, and 8.9%, respectively (Table S3, SI). UV–vis–NIR spectra were examined to corroborate the PLE results. Figure 1d confirms that (9,8) is the dominant (*n,m*) species in producing SWCNTs after prereluction at 500 °C. For two other prereluction conditions, absorption spectra also agree with the PLE results. Furthermore, an intense and narrow radial breathing mode (RBM) peak is observed at close to 209  $\text{cm}^{-1}$  under 785 and 633 nm excitation in Raman spectra (Figure 1e), which corresponds to (9,8) nanotubes.<sup>6</sup>

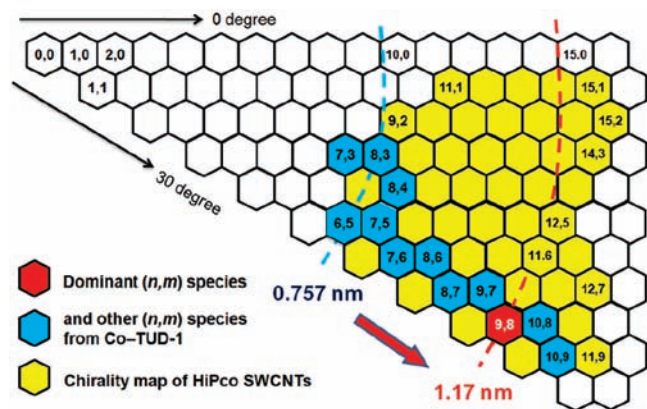


**Figure 2.** Chirality maps of SWCNTs grown from Co-TUD-1.

Prereluction temperature is a critical factor for achieving high selectivity toward (9,8) nanotubes. As illustrated in Figure 2, when Co-TUD-1 is reduced to 400 °C, major (*n,m*) species are at 0.757 nm. When the prereluction temperature is increased to 500 °C, (9,8) is 1.17 nm. Conversely, the catalyst loses its (*n,m*) selectivity when the prereluction temperature is further raised to 600 °C. The optimal prereluction temperature at 500 °C has strongly correlated with the TPR reduction temperature at 483 °C, as evidenced in Figure S2b, SI. We varied the SWCNT growth temperature under CO from 600 to 900 °C. The growth temperature between 600 to 800 °C only affected the carbon yield rather than (*n,m*) selectivity. When the growth temperature was higher than 850 °C, SWCNTs show a broad (*n,m*) distribution similar to that of HiPco nanotubes, regardless of the prereluction temperature.

Analogous to Co-MCM-41 catalyst,<sup>7</sup> Co species on TUD-1 can nucleate in two steps. First,  $\text{Co}^{2+}$  ions are partially reduced in  $\text{H}_2$  during prereluction, but they are still dispersed isolatedly on the large surface of TUD-1. Second, Co atoms aggregate quickly into clusters under CO to initiate SWCNT growth. The uniqueness of Co-TUD-1 relies on its low reduction temperature (483 °C vs 700–900 °C of Co-MCM-41), which increases the amount of reduced Co atoms available for forming Co clusters when CO is

introduced. At the same time, its large surface area and the strong metal–support interaction are sufficient in stabilizing these clusters with a narrow diameter distribution at around 1.2 nm, responsible for the growth of (9,8) nanotubes. If the prereluction temperature is too low, less reduced Co atoms are available, causing slightly smaller Co clusters to grow smaller diameter nanotubes, such as (6,5). On the other hand, if the prereluction temperature is too high, TUD-1 cannot stabilize the large amount of reduced Co atoms, and Co clusters with various sizes could form, which leads to the loss of (*n,m*) selectivity. We also notice the overall high selectivity toward large chiral angle nanotubes. Although some theoretical studies have tried to explain this,<sup>8</sup> more studies are required to provide a comprehensive explanation.

A motivation to control the (*n,m*) structure of larger diameter nanotubes is their potential improvement in electronic performances. SWCNT thin film FETs were fabricated using (9,8) nanotubes from Co-TUD-1 and (6,5) nanotubes from Co–Mo (see SI for details). Figures 3 and S7, Table S4, and SI demonstrate that semiconducting (9,8) devices have a higher average mobility than that of (6,5) devices (0.903 vs 0.135  $\text{cm}^2/(\text{V}\cdot\text{s})$ ). Smaller diameter SWCNTs are known to have poorer contacts and lower carrier mobilities.<sup>9</sup> Moreover, compared under similar nanotube densities and length distributions, a higher percentage of (9,8) devices have semiconducting characteristics ( $I_{\text{on}}/I_{\text{off}} > 10^3$ ) compared to (6,5) devices. (9,8) nanotubes from our synthesis process demonstrate superior FET device performance.

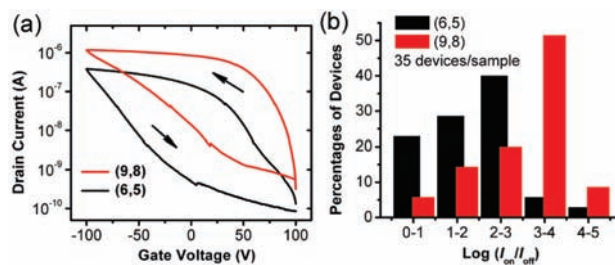


**Figure 3.** (a) Typical drain current-gate voltage curves of the thin film FETs from (9,8) and (6,5) SWCNTs. (b) Percentage histogram of FET on–off ratios from the two types of SWCNTs.

In conclusion, we have demonstrated that (9,8) nanotubes can be selectively grown. Prereluction in  $\text{H}_2$  at 500 °C results in 59.1% of semiconducting nanotubes having the (9,8) structure. Combining with further postsynthetic sorting techniques, our selective synthesis method brings us closer to the ultimate goal of producing (*n,m*) specific nanotube materials, which would have a profound impact in carbon nanotube electronic and optoelectronic technology.

**Acknowledgment.** We acknowledge financial support by NRF-CRP2-2007-02 from National Research Foundation, Singapore.

**Supporting Information Available:** Co-TUD-1 and SWCNT synthesis and characterization, FET device fabrication and characterization. This material is available free of charge via the Internet at <http://pubs.acs.org>.

## References

- Jorio, A.; Dresselhaus, G.; Dresselhaus, M. S., Eds. *Carbon Nanotubes, Advanced Topics in the Synthesis, Structure, Properties and Applications*; Springer: Berlin, 2008; p 735.
- (a) Bachtlo, S. M.; Balzano, L.; Herrera, J. E.; Pompeo, F.; Resasco, D. E.; Weisman, R. B. *J. Am. Chem. Soc.* **2003**, *125*, 11186–11187. (b) Miyauchi, Y.; Chiashi, S.; Murakami, Y.; Hayashida, Y.; Maruyama, S. *Chem. Phys. Lett.* **2004**, *360*, 229–234. (c) Ciuparu, D.; Chen, Y.; Lim, S.; Haller, G. L.; Pfefferle, L. *J. Phys. Chem. B* **2004**, *108*, 503–507. (d) Li, X.; Tu, X.; Zanic, S.; Welsher, K.; Seo, W. S.; Zhao, W.; Dai, H. *J. Am. Chem. Soc.* **2007**,

- 129, 15770–15771. (e) Chiang, W.-H.; Sankaran, R. M. *Nat. Mater.* **2009**, *8*, 882–886. (f) Ghorannevis, Z.; Kato, T.; Kaneko, T.; Hatakeyama, R. *J. Am. Chem. Soc.* **2010**, *132*, 9570–9572.
- (3) (a) Hersam, M. C. *Nat. Nanotechnol.* **2008**, *3*, 387–394. (b) Liu, J.; Hersam, M. C. *MRS Bull.* **2010**, *35*, 315–321.
- (4) Aquino, C.; Maschmeyer, T. A New Family of Mesoporous Oxides - Synthesis, Characterisation and Applications of TUD-1. In *Ordered Porous Solids Recent Advances and Prospects*; Valtchev, V., Mintova, S., Tsapatsis, M., Eds.; Elsevier Science: Oxford, 2009; pp 4–30.
- (5) O'Connell, M. J.; Bachilo, S. M.; Huffman, C. B.; Moore, V. C.; Strano, M. S.; Haroz, E. H.; Rialon, K. L.; Boul, P. J.; Noon, W. H.; Kittrell, C.; Ma, J. P.; Hauge, R. H.; Weisman, R. B.; Smalley, R. E. *Science* **2002**, *297*, 593–596.
- (6) Dresselhaus, M. S.; Dresselhaus, G.; Jorio, A. *J. Phys. Chem. C* **2007**, *111*, 17887–17893.
- (7) (a) Ciuparu, D.; Chen, Y.; Lim, S.; Yang, Y.; Haller, G. L.; Pfefferle, L. *J. Phys. Chem. B* **2004**, *108*, 15565–15571. (b) Ciuparu, D.; Haider, P.; Fernandez-Garcia, M.; Chen, Y.; Lim, S.; Haller, G. L.; Pfefferle, L. *J. Phys. Chem. B* **2005**, *109*, 16332–16339.
- (8) (a) Reich, S.; Li, L.; Robertson, J. *Chem. Phys. Lett.* **2006**, *421*, 469–472. (b) Ding, F.; Larsson, P.; Larsson, J. A.; Ahuja, R.; Duan, H. M.; Rosen, A.; Bolton, K. *Nano Lett.* **2008**, *8*, 463–468. (c) Ding, F.; Harutyunyan, A. R.; Yakobson, B. I. *Proc. Natl. Acad. Sci. U.S.A.* **2009**, *106*, 2506–2509.
- (9) Zhou, X.; Park, J. Y.; Huang, S.; Liu, J.; McEuen, P. L. *Phys. Rev. Lett.* **2005**, *95*, 146805.

JA106937Y